Supporting Information

The in-situ growth of atomically dispersed Ni species on CeO_2 during low-temperature CH_4/CO_2 reforming

Hui Wang[a,*], Yansu Hu[a], Alexander Adogwa,[b] Ming Yang[b,*], Tong-Bu Lu[a,*]

[a] Institute for New Energy Materials and Low Carbon Technologies, School of Materials Science and Engineering, Tianjin University of Technology, Tianjin 300384, China

[b] Department of Chemical and Biomolecular Engineering, Clemson University, Clemson, SC, 29634, USA

Corresponding Author

*wanghui2020@email.tjut.edu.cn; *myang3@clemson.edu; *lutongbu@tjut.edu.cn

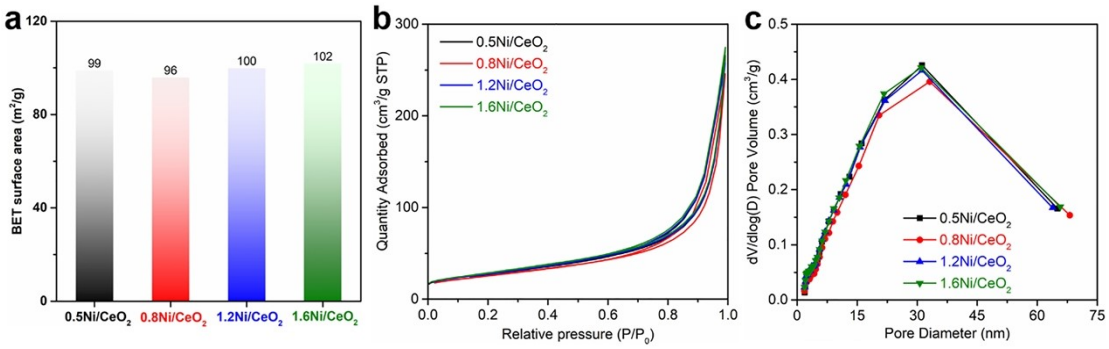

Fig. S1. The physical structures of Ni/CeO_2 catalysts with different Ni species. (a) BET surface area, (b) N_2 adsorption-desorption curves, and (c) the pore distribution curves of the four Ni/CeO_2 catalysts.

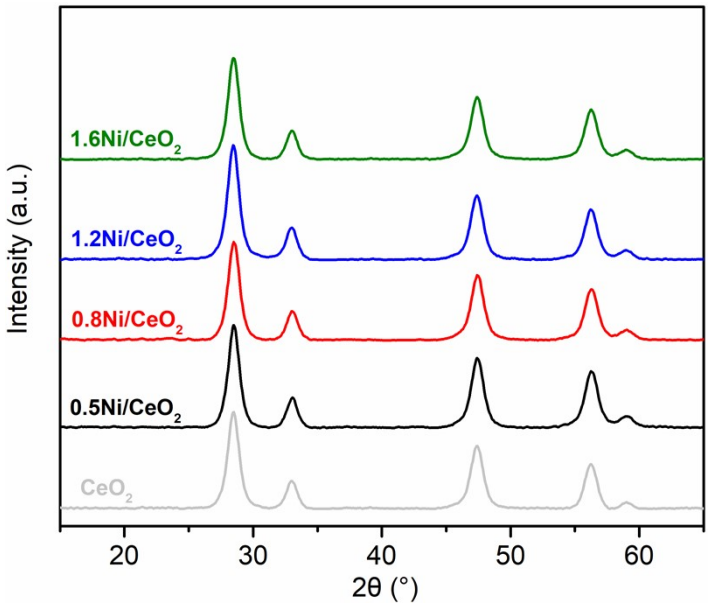

Fig. S2. XRD patterns of the as-prepared Ni-free ceria and Ni/CeO_2 catalysts. No Ni or NiO signal was detected.

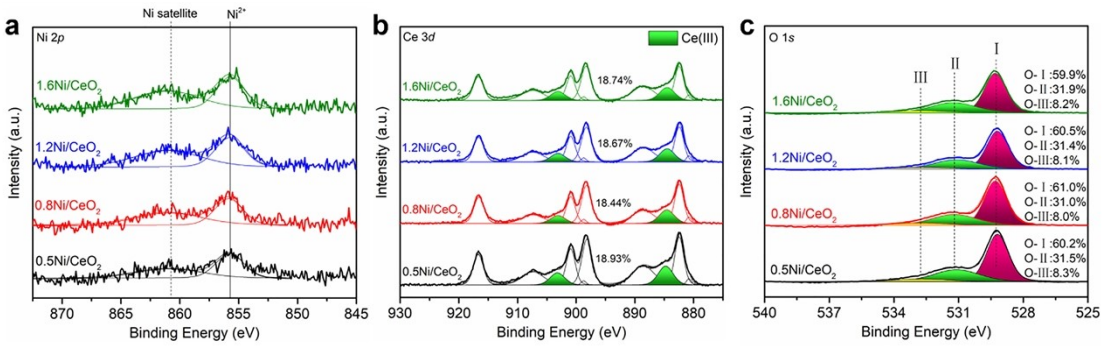

Fig. S3. XPS spectra of as-prepared Ni/CeO_2 samples. (a) Ni 2*p*, (b) Ce 3*d*, and (c) O 1*s* spectra of Ni/CeO_2 samples with different Ni loading amount.

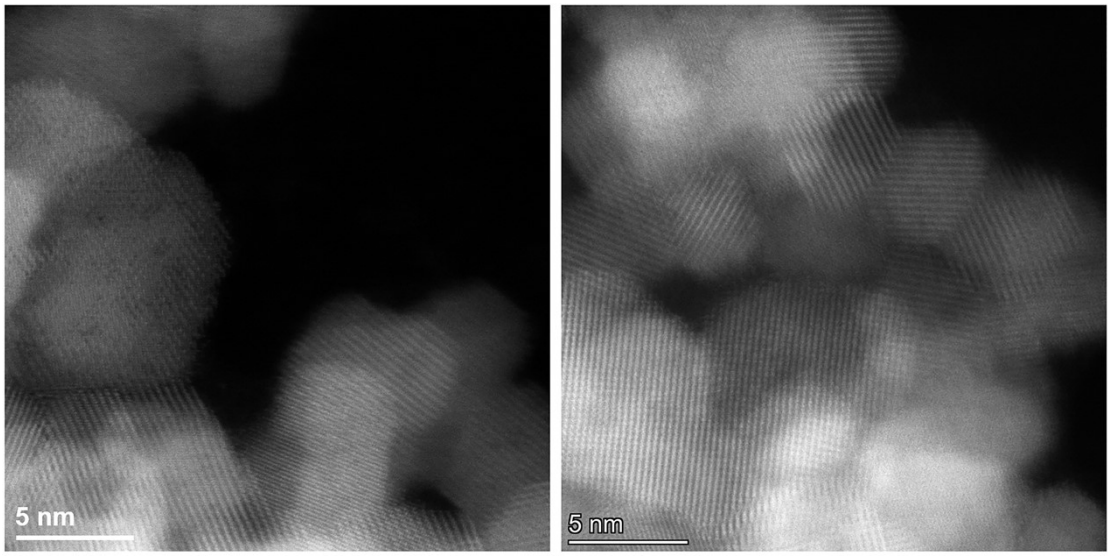

Fig. S4. Aberration-corrected HAADF-STEM images for the as-prepared 1.6Ni/CeO_2 catalyst. No obvious Ni NPs was observed. The left and right images are the two representative views.

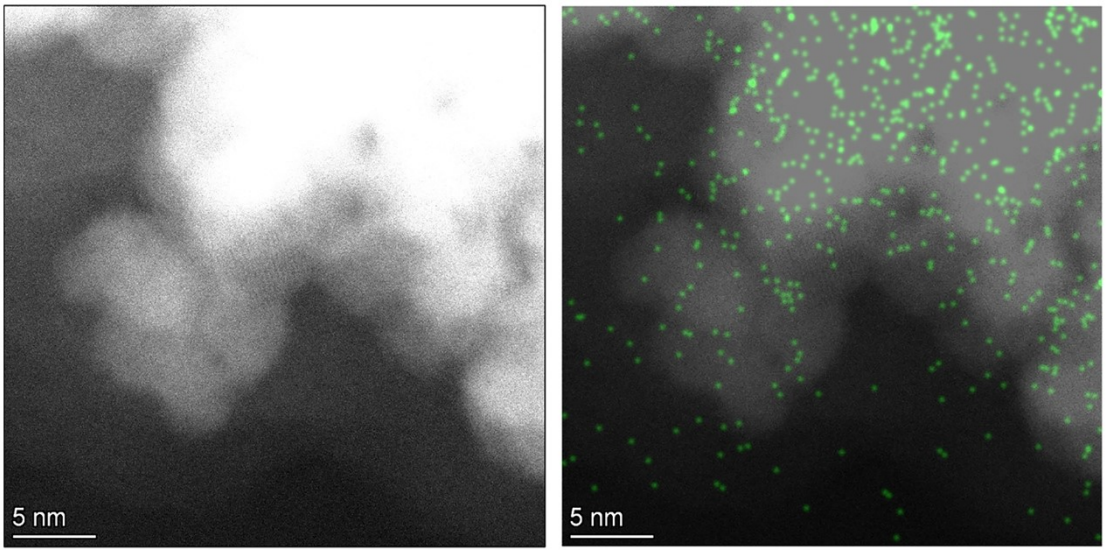

Fig. S5. Aberration-corrected HAADF-STEM image (left) and the corresponding EDS mapping (right) for the as-prepared 1.6Ni/CeO_2 catalyst. No obvious Ni NPs was observed. The green dot represents the Ni element.

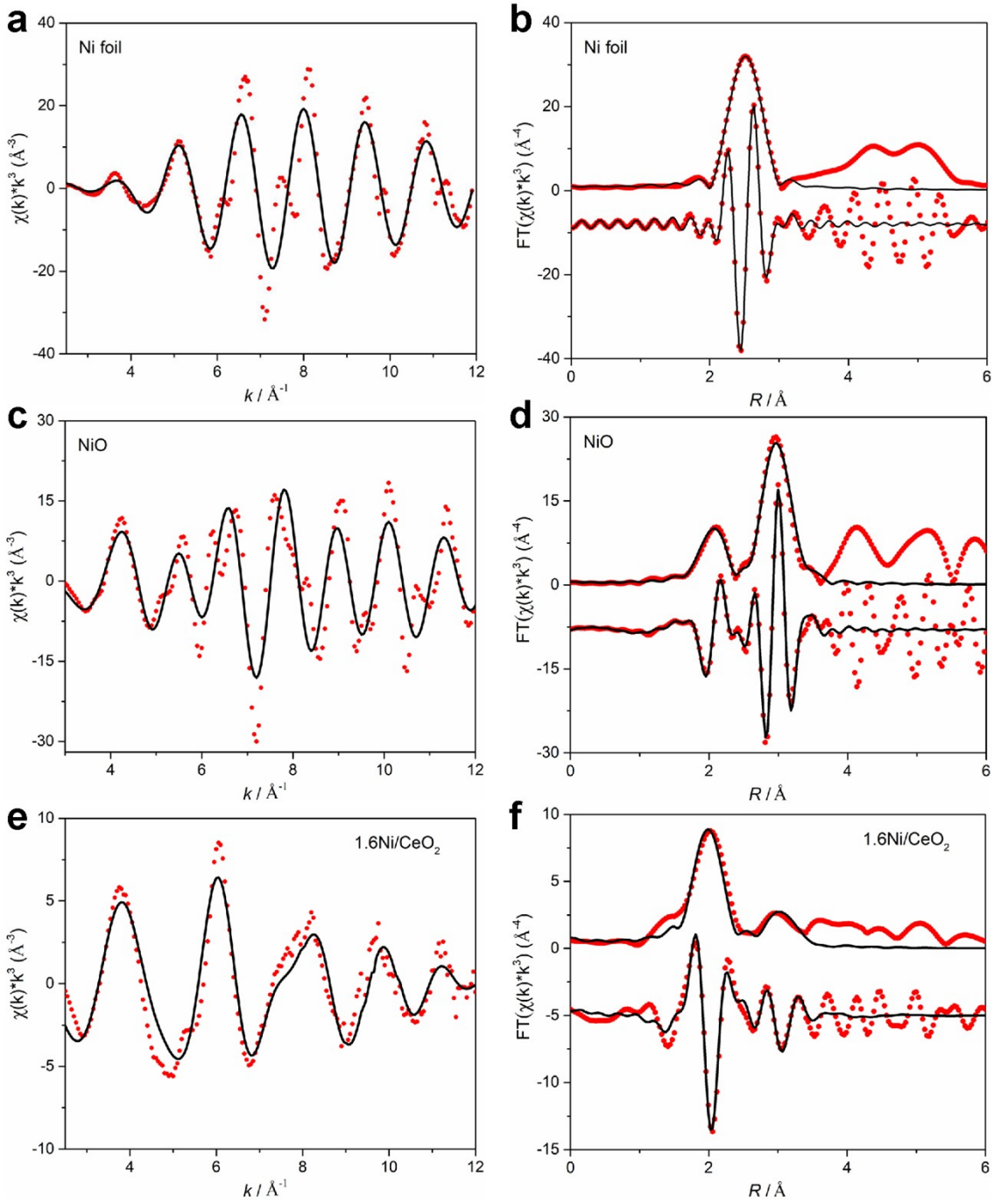

Fig. S6. Ni K-edge EXAFS (points) and curvefit (line) in k^3 weighted k-space (a, c, e) and R-space (FT magnitude and imaginary component, b, d, f). The data were phase-corrected.

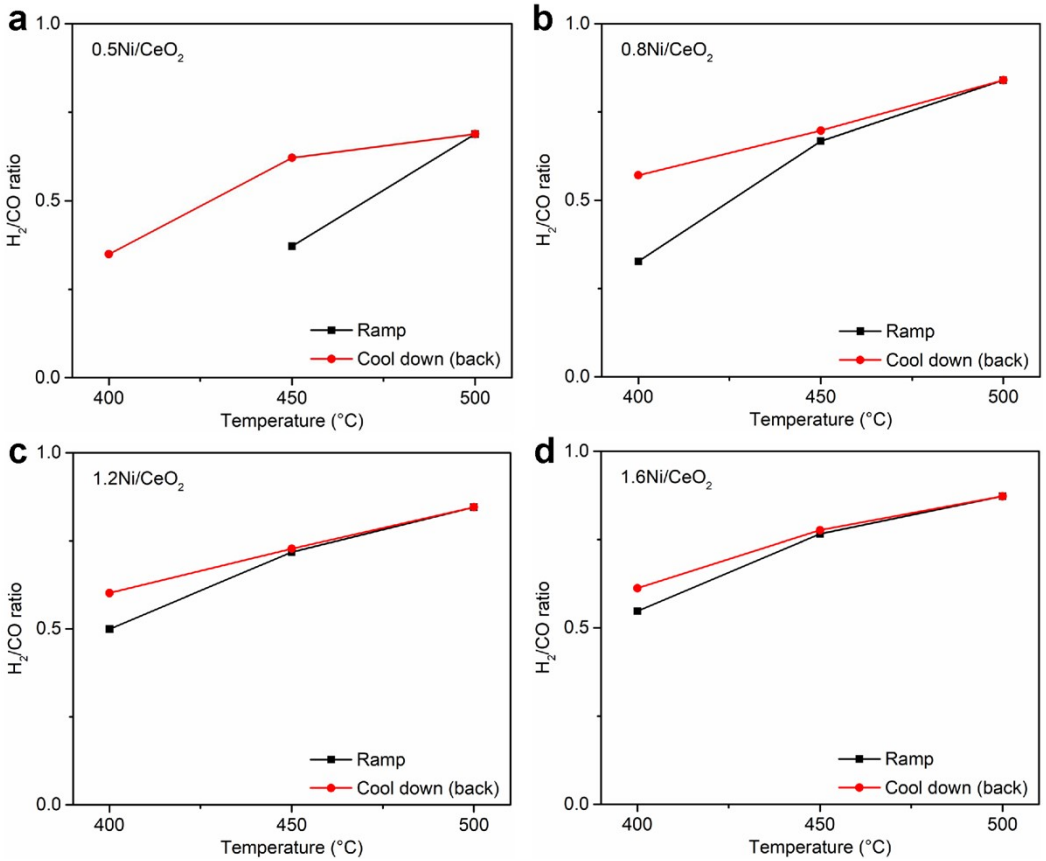

Fig. S7. The H_2/CO ratios of different Ni/CeO_2 catalysts during DRM reaction. The H_2/CO ratios during the ramping and cooling down (back) process of (a) 0.5Ni/CeO_2, (b) 0.8Ni/CeO_2, (c) 1.2Ni/CeO_2, and (d) 1.6Ni/CeO_2. These H_2/CO ratios correspond to the DRM catalytic performance in Fig. 5. Reaction conditions: [CH_4] = [CO_2] = 1%, balanced with N_2, contact time: 100,000 mL g_{cat}^{-1} h^{-1}.

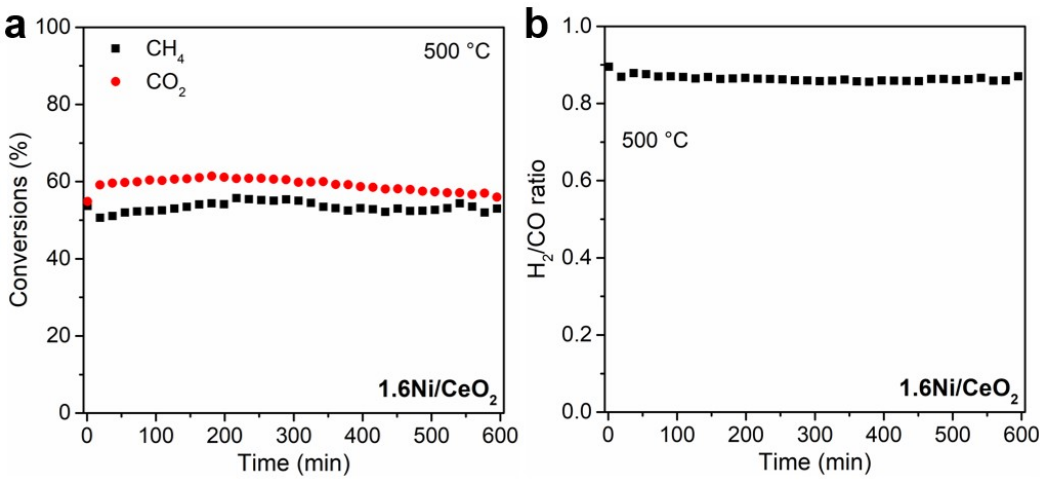

Fig. S8. DRM stability test at 500 °C for 1.6Ni/CeO_2 catalyst (a) Conversions of CH_4 and CO_2 (b) H_2/CO ratio (Reaction conditions: [CH_4] = [CO_2] = 1%, balanced with N_2, contact time: 25,000 mL $gcat^{-1}$ h^{-1}.)

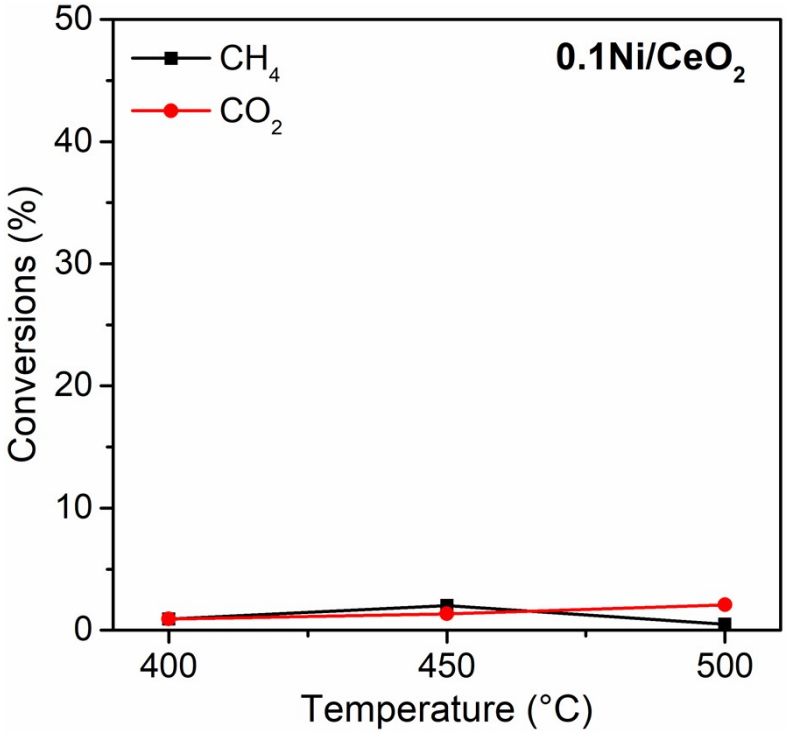

Fig. S9. DRM reaction test for $0.1Ni/CeO_2$ sample (Reaction conditions: $[CH_4] = [CO_2] = 1\%$, balanced with N_2, contact time: 25,000 mL $gcat^{-1}$ h^{-1}.)

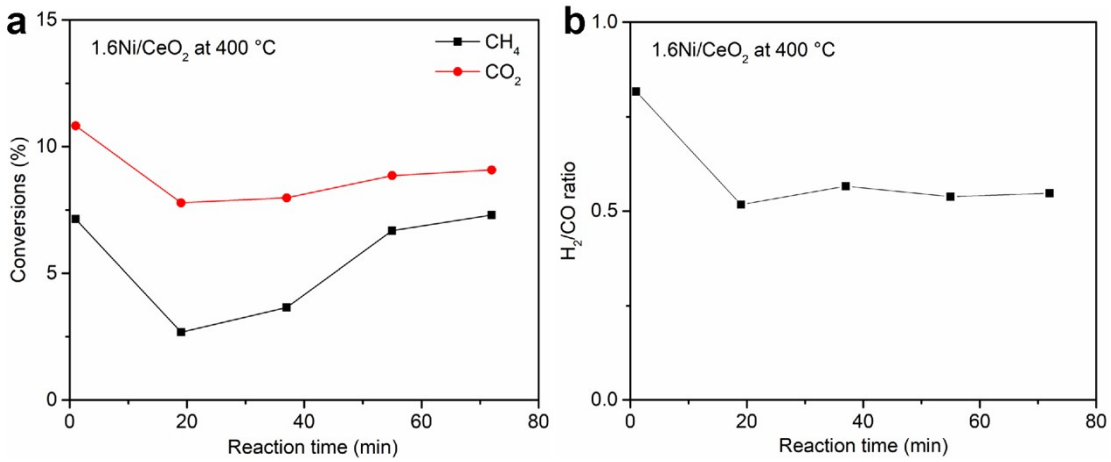

Fig. S10. DRM reactivity evolution of 1.6Ni/CeO_2 catalyst at 400 °C. (a) CH_4 & CO_2 conversions (b) H_2/CO ratio. Reaction conditions: [CH_4] = [CO_2] = 1%, balanced with N_2, contact time: 100,000 mL g_{cat}^{-1} h^{-1}.

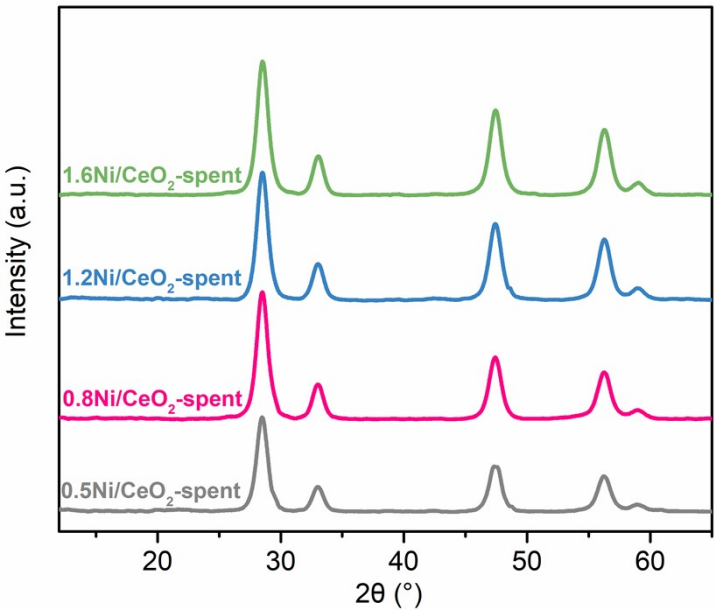

Fig. S11. XRD patterns of the reaction-spent Ni/CeO_2 catalysts. No Ni or NiO signal was detected.

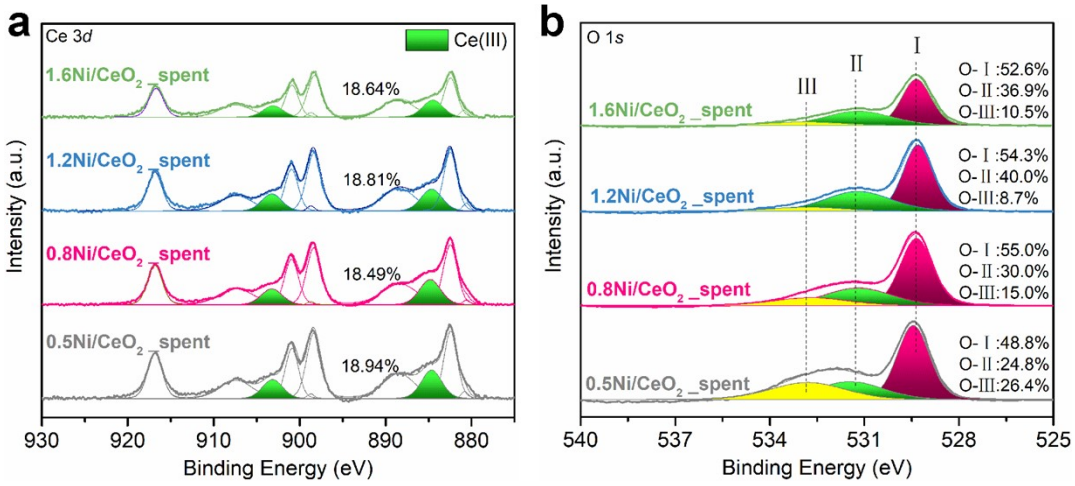

Fig. S12. XPS spectra of reaction-spent Ni/CeO_2 samples. (a) Ce 3*d*, and (b) O 1*s* spectra of Ni/CeO_2 samples with different Ni loading amount.

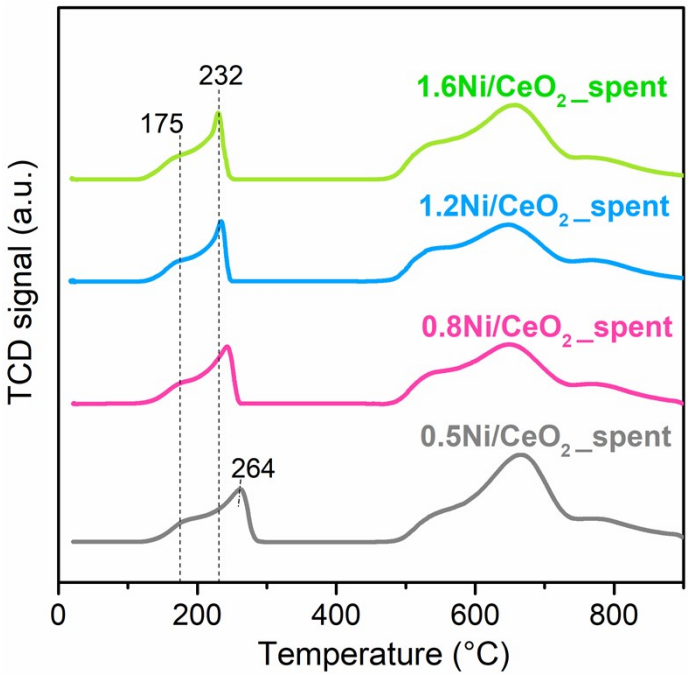

Fig. S13 H_2 TPR curves of the reaction-spent Ni/CeO_2 samples with different Ni loading amount.

The H_2 TPR curves below 300 °C are quite similar in shape, with all initial reduction peaks centered at 175 °C. This differs from the as-prepared counterparts, which exhibit significant discrepancy ranging from single atoms to nanoparticles (NPs) or clusters as Ni loading increases (Fig. 4). Additionally, the spent $0.5Ni/CeO_2$ shows a higher reduction temperature at the latter peak (264 °C), compared to 232 °C for the spent $1.2Ni/CeO_2$ and $1.6Ni/CeO_2$. Compared to the as-prepared samples (Fig. 4), all the reduction peaks have shifted to higher temperatures, likely due to carbon deposits. Based on the H_2 reduction attribution for the as-prepared Ni/CeO_2 catalysts (Fig. 4), where Ni NPs or clusters are preferentially reduced over single atoms, we conclude that there are still some Ni single atoms in the spent $0.5Ni/CeO_2$ sample. The spent $0.8Ni/CeO_2$ contains fewer Ni single atoms, while NPs or clusters predominate in the spent $1.2Ni/CeO_2$ and $1.6Ni/CeO_2$ catalysts.

Table S1 Fitting parameters of the curves fitted k^3-weighted EXAFS analyses at Ni K-edge.

Sample	Shell	CN	R (Å)	ΔE_0 (eV)	σ^2 (Å^2)	R-factor
Ni foil	Ni-Ni	12.0	2.48 ± 0.01	6.3 ± 1.1	0.002	0.01
NiO	Ni-O	5.7 ± 0.7	2.07 ± 0.03	9.3 ± 0.8	0.003	0.01
	Ni-O-Ni	13.2 ± 1.5	2.96 ± 0.02		0.005	
1.6Ni/CeO_2	Ni-O	6.7 ± 1.2	2.02 ± 0.08	6.5 ± 2.4	0.005	0.02
	Ni-Ce	4.0	3.03 ± 0.09		0.006	
		2.0	3.13 ± 0.02		0.006	

Note: Direct Ni-Ni contact does not exist in the 1.6Ni/CeO_2 sample. Amplitude reduction factor: S_0^2: 0.79 (obtained by analyzing the known Ni foil sample); CN, coordination number; R, the distance between absorber and backscattered atoms; ΔE_0, inner potential correction; σ^2, Debye-Waller factor, an evaluation for thermal and structural disorders; R-factor, closeness of the fit, if ≤ 0.02, consistent with broadly correct models.

Table S2 Ni dispersions of different Ni/CeO_2 catalysts after DRM reaction.

Catalysts	Ni dispersion (%)
$0.5Ni/CeO_2$-spent	51
$0.8Ni/CeO_2$-spent	50
$1.2Ni/CeO_2$-spent	47
$1.6Ni/CeO_2$-spent	48

Note: Ni dispersion was measured by CO chemisorption, and there is a CO_2 passivation for Ce^{3+} before CO pulse in. The ratio for CO: Ni was assumed to be 1:1. These reaction-spent Ni/CeO_2 catalysts suffered from the reaction from 400 to 500 °C with an interval of 50 °C and stayed for about an hour at each temperature point.

Table S3 TOF comparisons of various Ni-based catalysts reported in the literature and our work.

Samples	Ni loading (wt. %)	TOF (s^{-1})	Temperature (°C)	Note
0.5Ni/CeO_2	0.5	0.046	500	Our work
1.6Ni/CeO_2	1.6	0.049	500	
NiCe/SiO_2-A	5.67	0.064	500	[1]
Ni/SiO_2-A	6.75	0.045	500	
Ni/SiO_2-I	6.79	0.010	500	
Ni/CeO_2	5	0.018	500	[2]
3%-Ni/(NA-Al_2O_3)	3	0.054	500	[3]
5%-Ni/(NA-Al_2O_3)	5	0.049	500	
10%-Ni/(NA-Al_2O_3)	10	0.034	500	
20%-Ni/(NA-Al_2O_3)	20	0.017	500	
Ni/Mg(Al)O	12	0.045	500	[4]
Ni-Cu/Mg(Al)O(Cu/Ni=0.25)	12	0.050	500	
0.5Ni/CeO_2	0.5	0.031	450	Our work
1.6Ni/CeO_2	1.6	0.027	450	
Ni-Zr/SiO_2	8.3	0.004	450	[5]
Ni-Si/ZrO_2	7.8	0.008	450	
0.5Ni/CeO_2	0.5	0.006	400	Our work
1.6Ni/CeO_2	1.6	0.013	400	
Ni-Zr/SiO_2	8.3	0.001	400	[5]
Ni-Si/ZrO_2	7.8	0.003	400	
Ni@SiO_2@CeO_2		0.015	400	[6]
Ni@SiO_2		0.009	400	

Note: TOF values were calculated from the methane conversion and based on the total loading amount of Ni atoms. Here, we didn't involve Ni dispersion to avoid any experimental error from CO or H_2 chemisorption.

References

1 X. Zhao, M. Lu, H. Li, J. Fang, L. Shi and D. Zhang, *New J. Chem.*, 2017, **41**, 4869–4878.

2 M. Li and A. C. van Veen, *Appl. Catal. B Environ.*, 2018, **237**, 641–648.

3 S. Zhang, T. Yang, J. Yu, W. Zhan, L. Wang, Y. Guo and Y. Guo, *New J. Chem.*, 2021, **45**, 21750–21762.

4 K. Song, M. Lu, S. Xu, C. Chen, Y. Zhan, D. Li, C. Au, L. Jiang and K. Tomishige, *Appl. Catal. B Environ.*, 2018, **239**, 324–333.

5 Y. Wang, L. Yao, Y. Wang, S. Wang, Q. Zhao, D. Mao and C. Hu, *ACS Catal.*, 2018, **8**, 6495–6506.

6 K. Han, W. Yu, L. Xu, Z. Deng, H. Yu and F. Wang, *Fuel*, 2021, **291**, 120182.